

## A novel method for preparation of graphene-containing biochar and application to supercapacitors

X. Liu<sup>a</sup>, X. Ning<sup>a</sup>, B. Zeng<sup>b,\*</sup>, W. Liu<sup>b</sup>, L. Li<sup>b</sup>

<sup>a</sup>Hunan Provincial Key Laboratory of Fine Ceramics and Powder Materials, School of Materials and Environmental Engineering, Hunan University of Humanities, Science and Technology, Loudi, 417000, P. R. China

<sup>b</sup>College of Mechanical Engineering, Hunan University of Arts and Science, Changde 415000, P. R. China

New carbon-based materials have drawn tremendous attention in several technological applications. Here, the synthesis of graphene-containing biochar was prepared through carbonation and activation processes, using pre-oxidized magnolia flowers. In particular, the activation method was conducted in copper foil under high pressure, which led to the high biochar yield and excellent electrical conductivity of biochar for graphene-containing hybrid. Furthermore, heteroatoms (including nitrogen and oxygen) were successfully doped into the biochar. As a result, the hybrid demonstrated excellent electrical properties, at high nitrogen (1.02 %) and oxygen levels (14.80 %). The as-prepared biochar was used to produce an all solid state symmetric superconductor with a capacitance of  $261.8 \text{ F g}^{-1}$  at a specific current of  $0.5 \text{ A g}^{-1}$ , and energy density of  $6.9 \text{ Wh kg}_1$  at powder density of  $20 \text{ kW kg}^{-1}$ . The enhanced electrochemical performance was attributed to the positive effect of synergy between highly conductive graphene-containing biochar and heteroatoms doping.

(Received February 17, 2023; Accepted May 10, 2023)

*Keywords:* Magnolia flowers, Biochar; graphene, Supercapacitor

### 1. Introduction

With the increase in demand for energy, supercapacitors have recently gained extensive attention<sup>[1,2]</sup>. Biochar materials derived from biomass, have the characteristics of low-cost and environmental friendliness, which are suitable for the supercapacitor applications<sup>[3,4]</sup>. It is generally believed that suitable pore distribution in biochar favors the electric double-layer capacitance (EDLC) performance of the supercapacitor. Until now, the chemical activation method is regarded as one effective way to obtain these expected biochar materials. Li<sup>[5]</sup> et al. prepared biochar from pomelo peel using a chemical activation method, and the ratio of KOH/pomelo peel was 4:1. Lian<sup>[6]</sup> et al. synthesized biochar from pine cone and the results showed that, with KOH, activation ratio was increased from 2 : 1 to 4 : 1, thus, pore size of the biochar material was dimensionally transformed from small to larger micropores. Therefore, a major challenge with the current studies is the fact that the mass ratios of activation agents in the prepared biochar are high, and production is generally accompanied by the large waste of activation agent and resultant low biochar yield<sup>[7,8]</sup>.

In addition, the poor performance of biochar, resulting from inadequate electron conductivity<sup>[9,10]</sup>, limits its further applications. Incorporating conductive materials, such as carbon nanotubes<sup>[11]</sup>, graphene<sup>[12]</sup>, etc., into biochar is generally considered as an optimal strategy to enhance its properties. Among the electroactive materials, graphene has been extensively explored because of its intrinsic remarkable electrical and mechanical properties<sup>[13]</sup>. For instance, Chen<sup>[14]</sup> reported a composite of biochar/graphene by a one-step self-assembly method and obtained a hybrid structure, achieving a significantly improved areal capacitance of  $1625 \text{ mF cm}^{-2}$ . However, there are no current reports on biochar materials with excellent electrical conductivity, as well as high biochar yield, synthesized by activation method.

---

\* Corresponding author: 21467855@qq.com  
<https://doi.org/10.15251/DJNB.2023.182.603>

With respect to the preceding discussion, a novel activation method was adopted to mix powders of biomass and activation reagents (mass ratio of 1:1) and molded into a Cu foil under high pressure. The benefit of this method is not limited to a reduced amount of activation reagent to obtain higher yield of biochar, but also, excellent electrical properties of biochar, as a result of CVD-synthesized graphene embedded within the framework of the biochar. Furthermore, the reversible Faradaic reactions can be enhanced by doping the biochar with nitrogen (N) and oxygen (O). The as-prepared biochar was used to synthesize a solid state supercapacitor of capacitance of  $261.8 \text{ F g}^{-1}$  at a specific current of  $0.5 \text{ A g}^{-1}$ , and energy density of  $6.9 \text{ Wh kg}^{-1}$  at powder density of  $20 \text{ kW kg}^{-1}$ . Our finding provided a new method to synthesize high yield biochar and further its application in supercapacitor production.

## 2. Experimental details

### 2.1. Materials

The magnolia flowers were obtained from Loudi district of Hunan province. Polyvinyl alcohol (PVA, 1799), potassium hydroxide (KOH), concentrated sulfuric acid ( $\text{H}_2\text{SO}_4$ ) and concentrated hydrochloric acid (HCl) were purchased from Aladdin Co. Ltd.

### 2.2. Materials synthesis

50.0 g of magnolia flowers were cleaned by ultrasonic cleaning, and then heated in an oven at  $300 \text{ }^\circ\text{C}$  for 1 h. Afterwards, the obtained solid was crushed using a grinder ground and then mixed with KOH (mass ratio of 1 : 1). The obtained granules were wrapped by Cu foil and molded under a pressure of 5 MPa for 5 min. Here, KOH and magnolia pollen in copper foil formed a dense mixture before activation. The dried mixture was carbonized under nitrogen atmosphere at a rate of  $5 \text{ }^\circ\text{C}/\text{min}$  and heated to temperatures of  $700 \text{ }^\circ\text{C}$ ,  $800 \text{ }^\circ\text{C}$ , and  $900 \text{ }^\circ\text{C}$ , then held at these activation temperatures for 1 hour, and cooled to room temperature. Finally, the samples were washed with 1M HCl and rinsed with deionized water repeatedly, until the quality of the filtrate was close to neutral. Thereafter, the samples were labelled GC-700, GC-800, and GC-900, according to their activation temperatures. For comparison, the matched group carbonized under  $800 \text{ }^\circ\text{C}$  obtain from the simply mixing KOH with magnolia pollen was labeled C-800.

### 2.3. Materials characterization

The morphology of the carbon materials was investigated by Hitachi S4800 scanning electron microscopy (SEM) and JEM2100 transmission electron microscopy (TEM). The crystal structure was analyzed by X-ray diffraction (D8, ADVAHCL) with Cu  $K\alpha$  radiation. The chemical and electronic states of the sample surface were obtained through X-ray photoelectron spectroscopy measurements (XPS, Thermo K-Alpha). The graphitization degrees were measured by Raman spectrum (Renishaw, RM-1000).

### 2.4. Electrochemical measurements of electrodes

In a three-electrode system (reference electrode: saturated calomel electrode (SCE); counter electrode: platinum foil), the electrochemical evaluation of biochar was tested in 1 M  $\text{H}_2\text{SO}_4$  electrolyte. The working electrodes were conducted as follows: First, biochar was ground in a ball and sieved to a uniform size. Then, electroactive materials (85 wt. %), acetylene black (10 wt.%), PTFE binder (5 wt. %) were mixed using ethanol as a solvent and rolled into a thin sheet. It was cut into smaller pieces with dimensions of  $1 \text{ cm} \times 1 \text{ cm}$  and pressed on the stainless-steel mesh ( $1 \text{ cm} \times 1 \text{ cm}$ ), followed by vacuum drying in oven at  $60 \text{ }^\circ\text{C}$  for 24 h. The load mass of each electrode was approximately 5.0 mg. The electrochemical tests were performed on a CHI 760E electrochemical workstation. Electrochemical impedance spectroscopy (EIS) was performed in the frequency range of 0.01 to 100,000 Hz.

### 2.5. Electrochemical measurements of all-solid-state symmetric supercapacitors

A gel electrolyte was fabricated according to the following steps: PVA powder (1 g) was dissolved in 10 mL deionized water and stirred at 85 °C for 3 h. After cooling, H<sub>2</sub>SO<sub>4</sub> (1 g) was added, in a dropwise manner, to the above solution with constant stirring; thus, a PVA-H<sub>2</sub>SO<sub>4</sub> gel electrolyte was obtained. Electrode material was coated onto the surface of stainless-steel mesh, where the electroactive material area was 1 cm × 1 cm. Following vacuum drying in the oven at 60 °C for 24 h, two electrodes with the same mass loading (5 mg/cm<sup>2</sup>) were immersed into the PVA-H<sub>2</sub>SO<sub>4</sub> electrolyte for 0.5 h and then evaporated the excess water. The biochar electrode was prepared by the same method described earlier. Finally, an all-solid-state supercapacitor was fabricated by assembling a pair of biochar electrodes and PVA-H<sub>2</sub>SO<sub>4</sub> electrolyte as separator in a sandwich configuration.

The specific capacitance (*C*<sub>3s</sub> in the three-electrode system and *C*<sub>2s</sub> in the two-electrode device), energy density (*E*, Wh kg<sup>-1</sup>) and power density (*P*, W kg<sup>-1</sup>) of the symmetric supercapacitors are calculated from the galvanostatic discharge curve using the following equations:

$$C_{3s} = \frac{I \times \Delta t}{\Delta V \times m} \quad (1)$$

$$C_{2s} = \frac{2I \times \Delta t}{\Delta V \times m} \quad (2)$$

$$E = \frac{C_{2s} \times (\Delta V)^2}{4 \times 7.2} \quad (3)$$

$$P = \frac{3.6 \times E}{t} \quad (4)$$

where *I*,  $\Delta t$ ,  $\Delta V$ , *m* are the discharge current (A), discharge time (s), voltage window (V), and loading mass (g) of the active material on a single electrode, respectively.

### 3. Results and discussion

The structure of carbon products was analyzed by X-ray diffraction (XRD). As shown in Fig. 1a, two typically broad peaks at 25.0° and 43° of the four samples corresponded to the (002) and (101) planes of graphite, indicating an amorphous nature of all samples<sup>[15]</sup>. In addition, a relatively stronger peak at 43° for GC-800 implied the existence of more amount of graphene in the biochar samples<sup>[16]</sup>. Raman spectra reflected the defect feature of carbon materials and the two main peaks at 1350 cm<sup>-1</sup> (sp<sup>3</sup>-hybridized D peak) and 1585 cm<sup>-1</sup> (sp<sup>2</sup>-hybridized G peak) could be clearly seen<sup>[17]</sup>. The values of *I*<sub>D</sub>/*I*<sub>G</sub> of C-800, GC-700, GC-800, GC-900 was 1.23, 1.15, 1.08, 1.18, respectively, indicating that a high degree of graphitization is achieved by GC-800<sup>[18]</sup>. Furthermore, GC-700, GC-800 and GC-900 showed a faint 2D peak around 2700 cm<sup>-1</sup>, which strongly proved that graphene had integrated into the biochar frameworks during heat treatment in the copper foil<sup>[19]</sup>. Besides, the most obvious peaks of the 2D-peak for GC-800 implied the more amount of graphene in the biochar<sup>[20]</sup>. Therefore, improved electrical conductivity of biochar could be achieved and the high power for the pseudo-supercapacitors can be facilitated<sup>[21]</sup>.

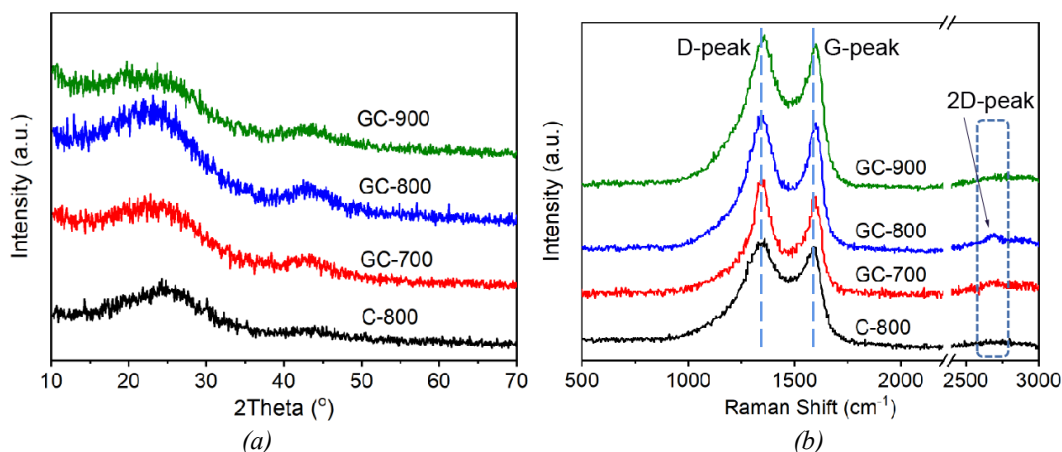


Fig. 1. (a) XRD pattern, (b) Raman spectra of the samples.

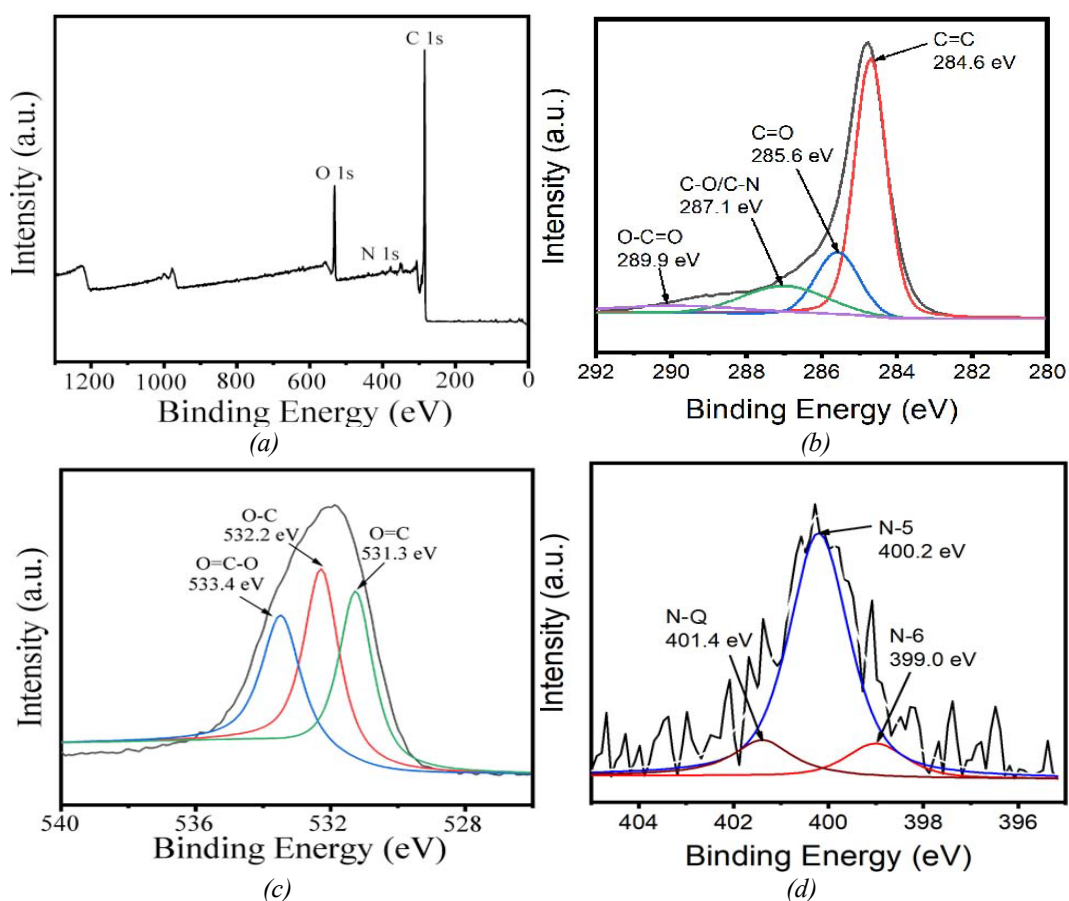


Fig. 2. XPS curves of the GC-800, (a) the survey spectra, (b) the C core level (1s) spectra, (c) the O core level (1s) spectra, (d) The N core level (2p) spectra.

XPS analysis of the GC-800 sample showed the characteristic peaks at 284.8 eV (C 1s), 400.1 eV (N 1s), and 532.6 eV (O 1s), implying the existence of C, O and N elements (Fig. 2a). From the result of XPS analysis, the atomic ratios of C, O, and N were 84.18%, 14.80%, and 1.02%, respectively. The deconvoluted C<sub>1s</sub> peaks showed four peaks, including C=C (284.6 eV), C=O (285.6 eV), C-N/C-O (287.1 eV), and O-C=O (289.9) (Fig. 2b). The amount of C=C bonds was approximately 80 at.%, and the rest of the C atoms existed in other forms of functional groups. These results confirmed that the frameworks were mainly filled with C atoms<sup>[22]</sup>. The deconvoluted

$O_{1s}$  peaks showed three peaks that included C=O (531.3 eV), C-O (532.2 eV), and O=C-O (533.4 eV), respectively, (Fig. 2c). The polar O-contained groups could favor the surface wettability and pseudo-capacitance<sup>[23]</sup>. The  $N_{1s}$  peak could be deconvoluted into three peaks at 399.0 eV, 400.2 eV, 401.4 eV (Fig. 4d), corresponding to pyridinic N (N-6), pyrrolic N (N-5), quaternary N (N-Q). The quaternary N favors the charge mobility and the pyridinic N with pyrrolic N could serve as a good electron-donor<sup>[24]</sup>. It proved that a certain amount of nitrogen and oxygen atoms have been successfully doped into the carbon surface, which could benefit for the electron transfer and the pseudo-capacitance of the carbon electrodes.

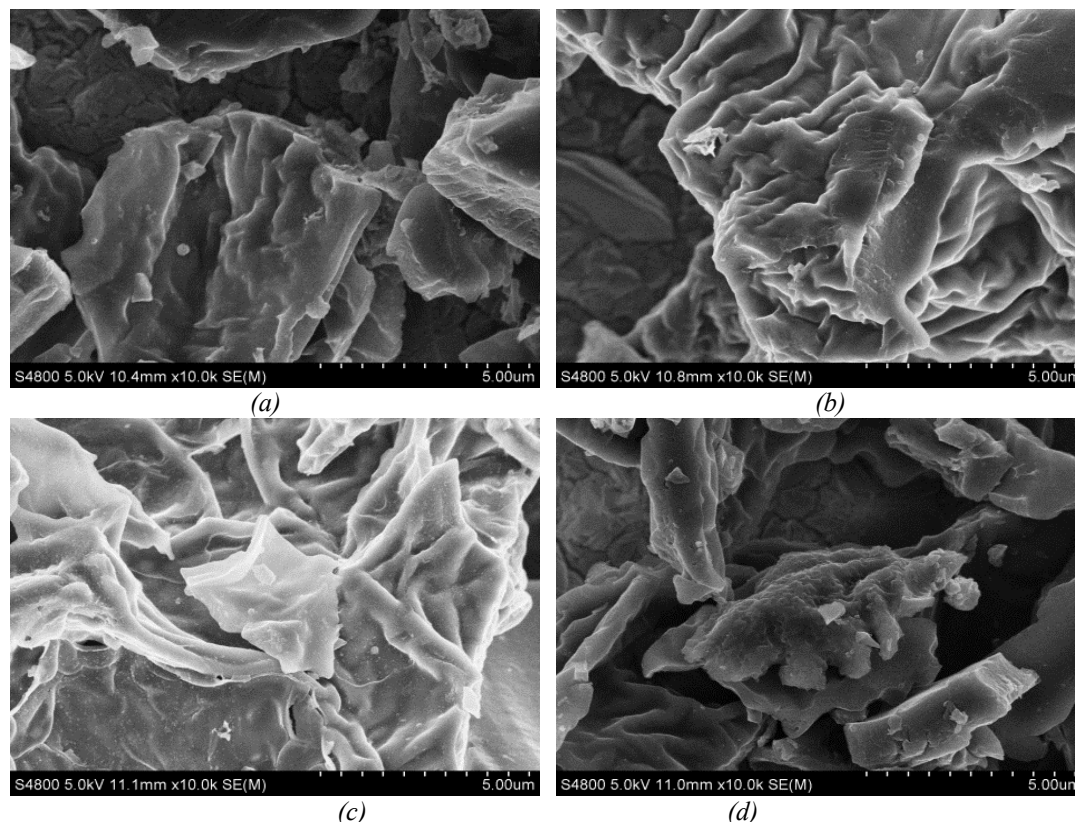


Fig. 3 SEM of (a) C-800, (b) GC-700, (c) GC-800, (d) GC-900 samples.

The morphology of the samples was investigated using scanning electron microscopic (SEM). As shown in Fig. 3a, C-800 exhibited a lumpy and laminar morphology with smooth surface. On the other hand, a wrinkled topography was observed on the surface of GC-700, which suggested the strongly connection between the active carbon and graphene layers, implying that graphene had grown in the biochar frameworks inside the copper foil. As the activation temperature increased to 800 °C, an increased fraction of wrinkled surface was observed, indicating the robust quantity of graphene in the bulk. However, with the increase of activation temperature to 900 °C, the smoother surface of the bulk indicated the decreasing content of graphene in the composites. All these results showed that activation process on the Cu foil led to the uniform growth of graphene in the biochar, which could contribute to the enhancement of electrical conductivity of biochar.

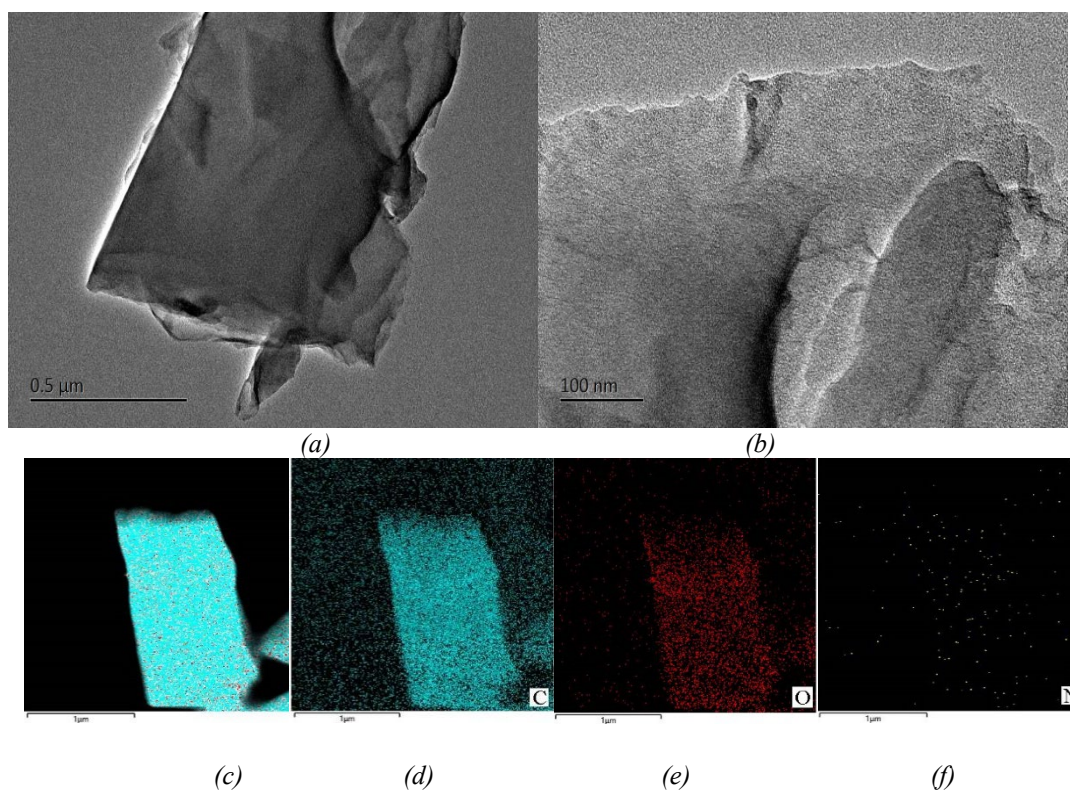


Fig. 4. (a) TEM images, (b) HRTEM lattice image, (c-f) elemental mapping images of GC-800.

Transmission electron microscopy (TEM) was employed to analyze the structural properties of GC-800. As shown in Fig. 4a, graphene sheets were tightly coated on the framework of the entire biochar, to provide a better electron conductive pathway and support electron transfer. No obvious lattice fringe in HRTEM images (Fig. 4b) indicated the amorphous carbon of biochar<sup>[25]</sup>. Energy dispersive X-ray spectrometry (EDS) mapping in Fig. 4c-f displayed the distribution of elements and it revealed that GC-800 was composed of C, O and N elements, further confirming the successful doping of O, N into the carbon framework. This type of meaningful structure was helpful to promote the electron transferring and improve the pseudo-capacitance.

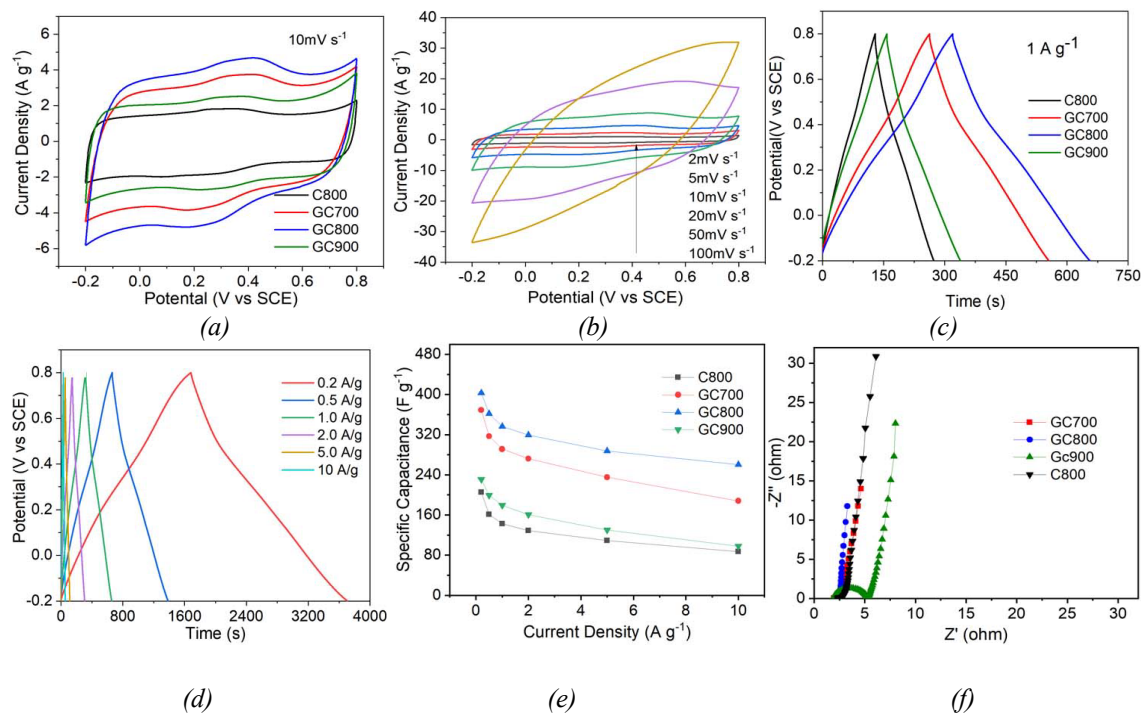


Fig. 5. Electrochemical performance of the samples in three-electrode systems: (a) CV curves of different samples at a scan rate of 100 mV s<sup>-1</sup>, (b) CV curves of GC-800 at different scan rates, (c) GCD curves of different samples at a various current density of 1 A g<sup>-1</sup>, (d) GCD curves of GC-800 at various current densities, (e) C3s at different current densities, (f) Nyquist plots of different samples electrodes.

Cyclic voltammetry (CV) was examined with a three-electrode system in 6 M KOH aqueous solution. As shown in Fig. 5a, all the CV curves of the electrode displayed a nearly rectangular curve, demonstrating that the EDL capacitance was the main form of the total capacitance<sup>[26]</sup>. Among them, GC-800 had the largest integrated area of the CV curve. It was suggested that the modification of biochar with highly interconnected graphene provided a significant improvement in the electron transport properties, resulting in facilitating electrolyte infiltration. Particularly at a high scan rate of 100 mV s<sup>-1</sup> (Fig. 5b), GC-800 still had an excellent rectangular shape, revealing outstanding rate performance and rapid charge-propagation capability. It could be also clearly seen that the discharge time of the GC-800 compound was much longer than the discharge times of C-800, GC-700 and GC-900 at the same current density (Fig. 5c). The high-rate capability supported high power density and their outstanding performance due to the strong adhesion of graphene onto biochar, facilitating a fast diffusion and transport for electrolyte ions. The charge-discharge profiles (Fig. 5d) of GC-800 showed highly symmetrical linearity, confirming its excellent electrochemical reversibility and good Columbic efficiency. As shown in Fig. 5e, the retentions of the specific capacitance of samples at 10 A g<sup>-1</sup> were 42.4% for C-800, 51.0% for GC-700, 64.6% for GC-800, and 42.4% for GC-900, respectively. Due to excellent electrical conductivity of graphene-containing biochar materials, it could enhance the electron transport capacity and improve the rate performance. Fig. 5f presented the Nyquist plots of the different samples. It was found that C-800 had the largest arc diameter in the high-frequency region, indicating its large charge transfer resistance (R<sub>ct</sub>). The Cu-coated biochar samples obtained (GC700, GC 800, and GC 900), showed smaller semicircle, which implied lower charge transfer resistance. The decrease in electrical resistance was caused by the formation of highly conductive graphene<sup>[27]</sup>.

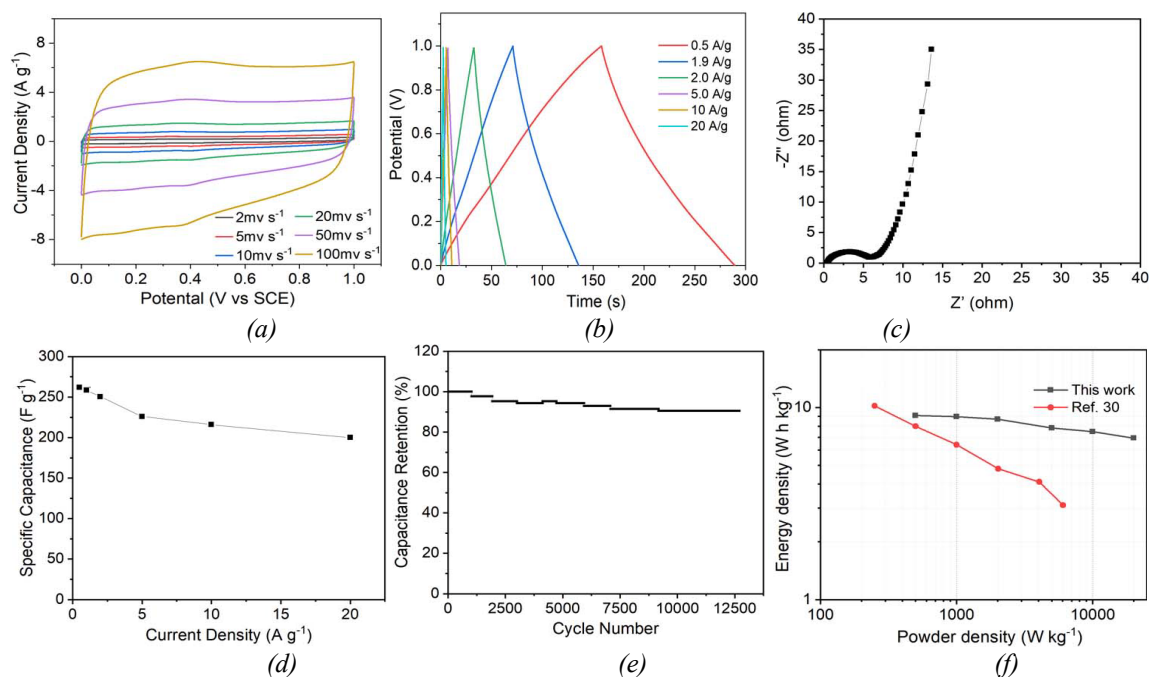


Fig. 6 Electrochemical performance of GC-800 based symmetric supercapacitors: (a) CV curves at different scan rates, (b) GCD curves at different current density, (c) Nyquist plot, (d) C2s at different current densities, (e) Cycle stability at 20 A g<sup>-1</sup>, (f) Ragone plot.

To further evaluate its potential for practical applications, two-electrode symmetric supercapacitors were assembled. As seen from Fig. 6a, when the scanning speed was increased, the CV curve remained similar to a rectangle, which indicated an adequate electrochemical reversible behavior<sup>[28]</sup>. At different scan rates, the GCD curves of GC-800 presented symmetrical triangular shapes (Fig. 6b), which indicated that the GC-800 presented ideal double-layer capacitance characteristics. The EIS line of device was nearly perpendicular to the actual axis (Fig. 6c) and the diameter of the semicircle related to the charge transfer resistance (Rct) was about 6 Ω; nearly similar to the ideal capacitor. The calculated specific capacitance, based on GCD curves illustrated in Fig. 6d, were 261.8, 258.4, 250.4, 226, 216 and 200 F g<sup>-1</sup> at a current density of 0.5, 1.0, 2.0, 5.0, 10 and 20 A g<sup>-1</sup>, respectively. The Nyquist plot was given in Fig. 6c. To evaluate the property of device, GCD test at 20 A g<sup>-1</sup> was conducted to characterize the long-term charge-discharge behavior. The specific capacitance retained 90% of the original capacity after 12500 cycles (Fig. 6e). Fig. 6f showed Ragone plots, which described the performance of the electronic energy storage devices. The specific energy density, based on supercapacitor, was calculated, and found to be about 9.1 Wh kg<sup>-1</sup> at 250 W kg<sup>-1</sup> and 6.9 Wh kg<sup>-1</sup> at 20 kW kg<sup>-1</sup>, which was higher than the values given in the Ref [30].

#### 4. Conclusions

In summary, graphene-containing biochar materials were synthesized using carbonation and activation process. The activation step was carried out in a Cu foil under high pressure, resulting to a high yield biochar with excellent electrical conductivity. The biochar exhibited both unparalleled gravimetric capacitance in aqueous electrolytes. The biochar GC-800 all-solid-state symmetric supercapacitor had a capacitance of 261.8 F g<sup>-1</sup> at 0.5 A g<sup>-1</sup>, and energy density of 6.9 Wh kg<sup>-1</sup> at powder density of 20 kW kg<sup>-1</sup>. The large capacitance performance could be attributed to excellent electrical conductivity of graphene-containing biochar and enhanced the reversible faradaic reactions by doping heteroatoms. This study offers a cost-saving method to fabricate a high-performance supercapacitor for practical application.

## Acknowledgments

This work was supported by the Natural Science Foundation of China (NSFC, No. 51802096), the Construct Program of the Key Discipline in Hunan Province and Project of the Natural Science Foundation of Hunan Province (2017JJ2191), Key project of Hunan Provincial Education Department (18A361) and the general project of Hunan Provincial Education Department (20C1258).

## References

- [1] H. Kareem, I.M. Ibrahim, S.J. Mohameed, et al., *Dig. J. Nanomater. Bios.* 16( 2), 493 (2021).
- [2] D.P. Chatterjee, A.K. Nandi. *J. Mater. Chem. A.* 9, 15880 (2021);  
<https://doi.org/10.1039/D1TA02505H>
- [3] X. Li, J. Zhang, B. Liu, Z. Su. *J. Clean. Prod.* 310(10), 127428 (2021);  
<https://doi.org/10.1016/j.jclepro.2021.127428>
- [4] B. Yan, J. Zheng, L. Feng, C. Du, et al., *Biochar.* 4, 50 (2022);  
<https://doi.org/10.1007/s42773-022-00176-9>
- [5] J. Li, W. Liu, D. Xiao, et al., *Appl. Surf. Sci.* 416, 918 (2017);  
<https://doi.org/10.1016/j.apsusc.2017.04.162>
- [6] M. Genovese, K. Lian. *J. Mater. Chem. A.* 5, 3939 (2017);  
<https://doi.org/10.1039/C6TA10382K>
- [7] F. Lü, X. Lu, S. Li, et al., *Chem. Eng. J.* 429(1), 132203 (2022);  
<https://doi.org/10.1016/j.cej.2021.132203>
- [8] P.S. Thue, D.R. Lima, E.C. Lima, et al., *J. Environ. Chem. Eng.* 10(3), 107632 (2022);  
<https://doi.org/10.1016/j.jece.2022.107632>
- [9] B. Rui, M. Yang, L. Zhang, et al., *J. Appl. Electrochem.* 50, 407 (2020);  
<https://doi.org/10.1007/s10800-020-01397-1>
- [10] D. Pontiroli, S. Scaravonati, G. Magnani, et al., *Micropor. Mesopor. Mater.* 285(1) 161 (2019); <https://doi.org/10.1016/j.micromeso.2019.05.002>
- [11] J. Zhang, A. Tahmasebi, J.E. Omoriyekomwan, et al., *Fuel process. Technol.* 213, 106714 (2021); <https://doi.org/10.1016/j.fuproc.2020.106714>
- [12] B. Rui, M. Yang, L. Zhang, et al., *J. Appl. Electrochem.* 50, 407 (2020);  
<https://doi.org/10.1007/s10800-020-01397-1>
- [13] Y. Sun, Y. Yuan, X. Geng, et al., *Carbon*, 199(31), 224 (2022);  
<https://doi.org/10.1016/j.carbon.2022.07.058>
- [14] R. Chen, X. Li, Q. Huang, et al., *Chem. Eng. J.* 412, 128755 (2021);  
<https://doi.org/10.1016/j.cej.2021.128755>
- [15] R. Gabhi, L. Basile, D.W. Kirk, et al., *Biochar*, 2, 369 (2020);  
<https://doi.org/10.1007/s42773-020-00056-0>
- [16] M. Zhang, B. Gao, Y. Yao, et al., *Sci. Total Environ.* 435(1), 567 (2012);  
<https://doi.org/10.1016/j.scitotenv.2012.07.038>
- [17] A. Ashraf, G. Liu, M. Arif, et al., *J. Clean. Prod.* 361(10), 132211 (2022);  
<https://doi.org/10.1016/j.jclepro.2022.132211>
- [18] B. Peng, L. Chen, C. Que, et al., *Sci. Rep.* 6, 31920 (2016);  
<https://doi.org/10.1038/srep31920>
- [19] Y. Wang, C. Srinivasakannan, H. Wang, et al., *Diam. Relat. Mater.* 125, 109034 (2022);  
<https://doi.org/10.1016/j.diamond.2022.109034>
- [20] Y. Zhang, B. Cao, L. Zhao, et al., *Appl. Surf. Sci.* 427(1), 147 (2018);  
<https://doi.org/10.1016/j.apsusc.2017.07.237>
- [21] B. Rui, M. Yang, L. Zhang, et al., *J. Appl. Electrochem.* 50, 407 (2020);  
<https://doi.org/10.1007/s10800-020-01397-1>

- [22] T. Chen, L. Luo, L. Luo, et al., *Renew. Energy*, 175, 760 (2021);  
<https://doi.org/10.1016/j.renene.2021.05.006>
- [23] G. Abdul, X. Zhu, B. Chen, et al., *Chem. Eng. J.* 319(1), 9 (2017).
- [24] S. Mandal, S. Pu, L. He, et al., *Environ. Pollut.* 259, 113851 (2020);  
<https://doi.org/10.1016/j.envpol.2019.113851>
- [25] Z. Luo, X. Zhu, J. Deng, et al., *J. Hazard.Mater.* 420(15), 126570 (2021);  
<https://doi.org/10.1016/j.jhazmat.2021.126570>
- [26] L.M. Dong, L. Chen, M.C. CAO, et al., *Dig. J. Nanomater. Bios.* 14(1), 7 (2019).
- [27] Z. Chen, K. Liu, S. Liu, et al., *Electrochim. Acta*, 237, 102 (2017);  
<https://doi.org/10.1016/j.electacta.2017.03.177>
- [28] J. Ren, L. Xia, Y. Zhou, et al., *carbon*, 140, 30 (2018);  
<https://doi.org/10.1016/j.carbon.2018.08.026>